International Journal of Pharmaceutics 522 (2017) 50–57

Contents lists available at ScienceDirect

International Journal of Pharmaceutics

journal homepage: www.elsevier.com/locate/ijpharm

Evaluation of a dynamic dissolution/permeation model: Mutual influence of dissolution and barrier-flux under non-steady state conditions

Daniel Sironi[a], Mette Christensen[a], Jörg Rosenberg[b], Annette Bauer-Brandl[a], Martin Brandl[a,*]

[a] Department of Physics, Chemistry and Pharmacy, University of Southern Denmark, Campusvej 55, DK-5230 Odense M, Denmark
[b] AbbVie GmbH & Co. KG, Knollstraße 50, D-67061 Ludwigshafen, Germany

ARTICLE INFO

Article history:
Received 27 October 2016
Received in revised form 28 February 2017
Accepted 1 March 2017
Available online 2 March 2017

Chemical compounds studied in this article:
Hydrocortisone (PubChem CID: 5754)

Keywords:
Hydrocortisone
Dissolution/permeation
Flux
Apparent permeability
Permeapad
Non-steady state

ABSTRACT

Combined dissolution/permeation testing is gaining increasing attention as an *in vitro* tool for predictive performance ranking of enabling oral formulations. The current aim was to study how *in vitro* drug permeation evolves under conditions, where the donor concentration is changing (non-steady state). To this end, a model case was construed: compacts of pure crystalline hydrocortisone methanolate (HC·MeOH) of slow release rates were prepared, and their dissolution and permeation determined simultaneously in a side-by-side setup, separated by a biomimetic barrier (Permeapad®). This was compared to a corresponding setup for a suspension of micronized hydrocortisone (HC). The HC suspension showed constant dissolved HC concentration and constant flux across the barrier, representing the permeation-limited situation. For the HC·MeOH compacts, various dynamic scenarios were observed, where dissolution rate and flux influenced each other. Interestingly, for all the dynamic scenarios, the incremental flux values obtained correlated nicely with the corresponding actual donor concentrations. Furthermore, donor depletion was tested using a HC solution. The dynamic interplay between decrease in donor concentration (down to less than 10% of the initial concentration) and flux was studied. The experiences gained are discussed in terms of further developing combined dissolution/permeation setups.

1. Introduction

The permeability of a drug compound is one of the determinants in the Biopharmaceutics Classification System (BCS) (Amidon et al., 1995). The classification of the compound into one of the four classes is one of the requirements for obtaining a BCS-based biowaiver for the final drug product. The preferred way for determining whether a compound has a high or a low permeability are pharmacokinetic studies in humans (FDA, 2015). Yet, it is also possible to determine the permeability using an appropriately validated setup with cell monolayers and reference substances. Therefore, permeability is often determined *in vitro* during late drug discovery/early drug development phase. In order to facilitate data evaluation, permeation experiments at this stage are typically designed to meet sink conditions, both in the donor and acceptor compartment. More precisely, the concentration in the acceptor compartment is kept virtually zero so that a significant contribution of back-diffusion can be ruled out. General consensus is that the acceptor concentration should be less than 10% of the donor concentration (Buckley et al., 2012).

Especially for solutions of compounds with limited aqueous solubility, a minor decay in donor concentration during the experiment may occur. A decay by up to 10 % is commonly considered as compatible with the sink-definition (Artursson, 1990).

In case of sink conditions, the steady state flux (J) of a drug across a permeation barrier can be derived from the linear part of the curve obtained when plotting the cumulative permeated amount vs. time (dQ/dt) following normalization by the permeation area (A) (Eq. (1)).

$$J = \frac{1}{A} \cdot \frac{dQ}{dt} \quad (1)$$

* Corresponding author.
E-mail address: mmb@sdu.dk (M. Brandl).

http://dx.doi.org/10.1016/j.ijpharm.2017.03.002
0378-5173/

Since, according to Fick's first law of diffusion, the flux is dependent on the concentration gradient, the steady state flux can be normalized by the initial concentration (c_0) and be reported as apparent permeability (P_{app}) in order to allow comparison of permeability data obtained with different experimental setups (Eq. (2)).

$$P_{app} = \frac{J}{c_0} \quad (2)$$

In a traditional permeability experiment (aiming for steady state permeation), a small permeation area and a large acceptor and donor compartment are basically beneficial for maintaining both sink conditions and a constant donor concentration.

On the other hand, there are a number of permeation-approaches described in literature, where the drug in the donor compartment is not present in dissolved state, but in solid state or in the form of a drug formulation or dosage form. These experiments are not intended to have any regulatory relevance but rather to give mechanistic insights or to allow a performance ranking of different formulations. To this end, there have been approaches suggested, which combine dissolution and Caco-2 permeation testing. Polli et al. transferred samples from a pharmacopeial paddle dissolution test of various tablets at a distinct time point to the donor compartment of a Caco-2 permeation setup (Ginski and Polli, 1999), or continuously circulated medium between dissolution and donor compartment (Ginski et al., 1999). Lehr at al. combined a pharmacopeial flow-through dissolution cell with Caco-2 and tested immediate release dosage forms (Motz et al., 2007). Yamashita et al. used a classical side-by-side diffusion setup and introduced griseofulvin in solid state, corresponding to 1% of the clinical dose, to the 8 mL donor chamber and followed its dissolution and permeation across the Caco-2 barrier simultaneously (Kataoka et al., 2003). During a series of follow-up studies using the same setup, they evaluated a number of influence factors e.g. food intake (Kataoka et al., 2006, 2011). More recent approaches employ non-cellular biomimetic barriers for the same purpose in order to overcome the limitations of cellular screens in terms of sensitivity against salts, inactive ingredients and biomimetic media (Fischer et al., 2011, 2012; Gantzsch et al., 2014).

In contrast, another type of dissolution/permeation setups employs (non-biomimetic) dialysis membranes to separate the donor (dissolution) from the acceptor compartment. Lovering and Black already pointed out in their pioneering work (Lovering and Black, 1973) that hydrophilic polydimethylsiloxane dialysis membranes are useful to determine the permeable fraction during a dissolution experiment and may thus help to predict intestinal absorption for a series of similar drugs, provided the drug compound does not interact with the membrane. Amphiphilic weak bases and acids, however, tend to interact with biomimetic membranes in response to their pH-dependent change in lipophilicity, a feature which cannot be captured by simple dialysis screens (Bibi et al., 2016). In recent decades considerably more sophisticated dialysis-based dissolution/permeation models have been designed, like the TNO model of dynamic gastric and intestinal transit and absorption, which is being used for drug studies (Blanquet et al., 2004), yet with the aforementioned limitation.

Finally, there is third group of non-sink dissolution approaches, where the dissolution compartment is supplemented by an absorptive sink-compartment consisting of octanol or similar non-water-miscible organic solvents, also addressed as biphasic dissolution. For a comprehensive review over biphasic systems see (Phillips et al., 2012).

With the advent of a large fraction of poorly water-soluble drug compounds in the pipelines of pharmaceutical industry and the inherent need for enabling formulations (Ku and Dulin, 2012), these types of non-steady state permeation settings are gaining increasing attention. Combined dissolution/permeation testing allowed, for instance, to identify the different underlying mechanisms of the enhanced permeation rate of a micro- and a nanoparticle formulation of fenofibrate (Sironi et al., 2017). Furthermore, combined dissolution/permeation testing has proven to be useful for estimating the food effect and the effect of the dose strength (Kataoka et al., 2011). Introducing an absorptive compartment is also useful for predicting the bioavailability in cases where precipitation plays an important role (Bevernage et al., 2012; Frank et al., 2014).

When combining dissolution testing with permeation studies, the donor concentration is subject to continuous changes, eventually in excess of the aforementioned limits. The donor and acceptor profiles are dynamically interrelated, and complex profiles are, hence, to be expected. Non-steady state conditions are e.g. given when the dissolution of the drug progresses slowly and thus may be rate-limiting for the overall process, or in cases where depletion of the donor compartment occurs. In consequence, there is limited information on how the geometry of such a combined dissolution/permeation setup should look like in order to render it appropriate to predict the *in vivo* behavior of (enabling) formulations.

The aim of this study was thus to explore the capabilities and limitations of a side-by-side (Ussing chamber) dissolution/permeation setup, equipped with a biomimetic barrier (Permeapad®). During a previous study (Sironi et al., 2017), the dissolution rates of the drug formulations used were rather high, and therefore, steady state permeation (constant flux) was observed in all cases (after an initial lag phase), which is regarded inappropriate for drugs, the biopharmaceutical behavior of which is expected to be solubility-/dissolution-rate-compromised. In order to better see the interplay between dissolution and permeation, a simplified model case was construed, where the dissolution rate is comparably low. Moreover, the dissolved drug was exclusively present in the molecularly dissolved state, i.e. not associated with micelles or other solubility-enhancing supramolecular assemblies (Fischer et al., 2011; Flaten et al., 2008).

Hydrocortisone (HC) was chosen as poorly soluble model drug with high permeability (BCS class II), and in order to reduce the dissolution rate, large crystals of hydrocortisone methanolate (HC·MeOH) were prepared. HC·MeOH was compressed without the use of excipients to compacts, and in some cases the tablets were partially covered with hard paraffin to further reduce the surface exposed to dissolution medium.

2. Material and methods

2.1. Chemicals

Hydrocortisone (micronized, Ph. Eur. 8.0, lot 15021106) and hard paraffin (Ph. Eur. 8.0) were purchased from Caesar & Loretz GmbH (Hilden, Germany). Highly purified water was prepared in-house using a Milli-Q® water purification system (Merck Millipore, Darmstadt, Germany). Methanol, ethanol and buffer salts were purchased from Sigma-Aldrich ApS (Brøndby, Denmark).

2.2. Media

Phosphate-buffered saline (PBS) contained 1.73 g L^{-1} of sodium dihydrogen phosphate dihydrate and 4.92 g L^{-1} disodium hydrogen phosphate dodecahydrate in highly purified water. The pH was adjusted with sodium hydroxide to a value between 7.35 and 7.45; the osmolality was adjusted with sodium chloride to a value between 280 and 290 mOsmol kg^{-1}.

2.3. Quantification of hydrocortisone

HC was quantified with UV/VIS spectroscopy at a wavelength of 248 nm using either a GENESYS 10 UV–scanning spectrophotometer (Thermo Fisher Scientific Inc., Waltham, Massachusetts, USA) or a FLUOstar Omega microplate reader (BMG LABTECH GmbH, Ortenberg, Germany) in connection with a 96 well Costar® titer plate (Corning Inc., Corning, NY, USA). The respective standard curves were prepared in the range from 1 $\mu g\,mL^{-1}$ to 100 $\mu g\,mL^{-1}$ and all samples were diluted appropriately with PBS. An additional standard curve was prepared with 96% ethanol for determining the recovery after the long-term depletion experiment.

2.4. Preparation of hydrocortisone methanolate

HC·MeOH was prepared according to a modified protocol (Chen et al., 2008; Fong et al., 2017). In brief, HC was dissolved in methanol at 50 °C under agitation. The solution was filtered through filter paper and stored at room temperature in a crystallizing dish with a pierced film cover until crystals formed.

2.5. Determination of the intrinsic dissolution rate

The intrinsic dissolution rate (IDR) of HC and respectively HC·MeOH in PBS was determined in a compendial dissolution tester (PTWS 310, Pharma Test Apparatebau AG, Hainburg, Germany) using the rotating disk method (Wood's apparatus; Ph. Eur. 8). Compacts with a surface area of 0.50 cm^2 were produced by compressing 100 mg of each powder with a hydraulic press at 300 MPa. Dissolution rate was tested in 500 mL of degassed PBS at 37 °C and 100 rpm. Samples of 2 mL were withdrawn every 10–30 min and replaced with fresh PBS. The total time for each experiment was 3.5 h.

2.6. Determination of equilibrium solubility

An excess of HC or HC·MeOH was dispersed in PBS and shaken for four days in a shaking water bath at 37 °C and 100 rpm (SW23, JULABO GmbH, Seelbach, Germany). After 24 h, 48 h, 72 h, and 96 h, an aliquot of 3.5 mL was filtered through a 0.45 μm pore-size cellulose acetate syringe filter (Sartorius AG, Göttingen, Germany) discarding the initial 3 mL of filtrate.

2.7. Preparation of hydrocortisone tablets

Tablets of pure HC·MeOH were prepared by compression in a single punch tablet press (EK0, KORSCH AG, Berlin, Germany) with a die diameter of 5 mm. Subsequently, the tablets were partially covered with solid paraffin in order to obtain a formulation with a constant release: solid paraffin was molten and poured on top of the tablet, leaving only the bottom surface uncovered.

2.8. Preparation of biomimetic permeation barrier Permeapad®

The biomimetic barrier was prepared as previously described (Di Cagno et al., 2015; Di Cagno and Bauer-Brandl, 2016). In brief, a thin layer of soy phosphatidylcholine (S-100) was applied to a hydrophilic support sheet (Pütz GmbH, Taunusstein, Germany). The final barrier (in use) was composed of hydrated lipid and support layer.

2.9. Dissolution/permeation study with a suspension of micronized hydrocortisone

The apparent permeability of HC was determined by employing a suspension of HC in PBS in a pair of jacketed side-by-side diffusion cells (PermeGear Inc., Hellertown, PA, USA). The volume of the donor compartment was 7 mL, and the volume of the acceptor compartment was 6 mL. Permeapad® was employed as biomimetic permeation barrier, and the effective permeation area was 1.77 cm^2. PBS was used as acceptor medium, and both the donor and the acceptor compartment were stirred with the provided cross-shaped stirbars at a fixed speed of 500 rpm (H-3 stirrer, PermeGear Inc., Hellertown, PA, USA). In order to maintain sink conditions in the acceptor chamber, samples of 2 mL were taken and replaced with fresh medium after pre-defined time intervals. This experiment was performed at 25 °C and 37 °C; all following experiments were performed at 37 °C and are summarized in Table 1.

2.10. Dissolution/permeation studies with tablets

Combined dissolution/permeation studies were performed by placing a tablet in the rear part of the donor cell before assembly. After pre-defined time intervals, samples were taken from both the acceptor and the donor compartment. Two different donor sampling regimes were tested for the uncovered tablets: 20 μL without volume replacement (i.e. no influence on the donor concentration) and 1 mL with replacement by fresh buffer (i.e. dilution). For all other experiments, 20 μL was chosen as sample volume. Filtration was not necessary as the tablets did not disintegrate.

2.11. Depletion experiments

The rate of depletion of the donor compartment (as a consequence of drug permeation) was determined by employing HC solutions of different concentrations in the aforementioned permeation setup. Samples of 20 μL were taken from the donor, and each experiment was run over 6 h.

The depletion of the donor was further tested with a highly concentrated solution (288.7 $\mu g\,mL^{-1}$) over 94.5 h. In order to maintain the concentration in the acceptor below 10% of the donor concentration regardless of the sampling frequency, the acceptor was operated in flow-through mode: the acceptor volume of the

Table 1
Summary of experimental conditions of the permeation and dissolution/permeation experiments.

Modification	Formulation	Donor volume [mL]	Volume of donor samples [mL]	Donor sample replacement	Acceptor volume [mlL	Volume of acceptor samples [mL]	Steady state permeation
Micronized HC	Saturated suspension	7	–	–	6	2	Yes
HC·MeOH	Tablet	7	1	Yes	6	2	No
	Tablet	7	0.02	No	6	2	No
	Covered tablet	7	0.02	No	6	2	No
(Micronized HC)	Solution	7	0.02	No	6	2	Yes
	Solution	7	0.02	No	(Flow-through)	–	No

side-by-side diffusion cell was continuously replaced by fresh PBS using a peristaltic pump (ECOLINE VC-MS/CA8-6, Cole-Parmer GmbH, Wertheim, Germany). The flow rate was 12.5 mL h^{-1} and fractions were collected at pre-determined time points over a sampling time of 1 min each. The flow rate was determined before and after the experiment (data not shown). The barrier was dissolved in 3 mL ethanol after the experiment in order to quantify drug that may have accumulated in the barrier.

2.12. Evaluation of permeation experiments

Steady state flux values were calculated from the respective slope of the regression line obtained by plotting the cumulative amount of permeated drug normalized by the permeation area vs. time (Eq. (1)). The apparent permeability was calculated for the suspension according to Eq. (2).

For the long-term depletion experiment with decaying donor concentration and an acceptor compartment operated in flow-through mode, flux at each given time point (J_t) was calculated from the acceptor concentration ($c_{Acceptor,t}$) at the same time point and the flow rate (ν) according to Eq. (3).

$$J_t = \frac{c_{Acceptor,t} \cdot \nu}{A} \tag{3}$$

For further evaluation regarding the relationship between (changing) donor concentrations and the observed permeation over time, the incremental permeation was derived from the measured donor profile. Under the assumption that the acceptor concentration at all time points is negligible, the depletion of the donor follows an exponential decay over time as shown in Eq. (4),

$$c_t = c_0 \cdot e^{-k \cdot t} \tag{4}$$

where c_0 is the initial concentration and k is the decay constant. The decay constant depends on the fraction x of the amount of drug present in the donor that permeates from the donor into the acceptor per time unit. It is commonly derived from the permeation area and the donor volume (V_{Donor}) of the experimental setup (Eq. (5)).

$$x = P_{app} \cdot \frac{A}{V_{Donor}} \tag{5}$$

The amount present in the donor at a given time can be described as follows (Eq. (6)):

$$c_t = c_0 \cdot (1 - x)^t \tag{6}$$

The combination of Eqs. (5) and (6) finally leads to Eq. (7).

$$c_t = c_0 \cdot e^{\ln\left(1 - P_{app} \cdot \frac{A}{V}\right) \cdot t} \tag{7}$$

2.13. Prediction of acceptor and donor profiles

In the case of the dissolution/permeation experiments with tablets, an interval-based approach was chosen in order to derive the permeation profiles from the dissolution curve: assuming that the flux is constant within each sampling interval (Δt), the flux and subsequently the permeated amount were calculated for each interval with Eq. (8).

$$\Delta Q = A \cdot P_{app} \cdot c_{Donor,t} \cdot \Delta t \tag{8}$$

Individual permeation profiles were calculated from each of the dissolution profiles and, subsequently, means and standard deviations were calculated. In the case of the covered tablets, outliers (visually determined) were replaced by the arithmetic mean of the concentration before and after the respective time point for calculating the flux.

2.14. Statistical analysis

For comparison of data sets, an unpaired, two-tailed Student's t-test was applied. A value of $p \leq 0.05$ was considered as significantly different.

3. Results and discussion

3.1. Intrinsic dissolution rate and equilibrium solubility of hydrocortisone and hydrocortisone methanolate

The release from the compressed HC and HC·MeOH was linear over the whole course of the IDR experiment, and no significant difference was found between the two modifications under these conditions (0.032 ± 0.003 mg min^{-1} cm^{-2} for HC vs. 0.030 ± 0.002 mg min^{-1} cm^{-2} for HC·MeOH).

Equilibrium solubility of micronized HC was determined to be 319.4 ± 12.1 µg mL^{-1} and was reached within three days under the conditions employed (no significant difference between day three and four). In the case of HC·MeOH, equilibrium was not (yet) reached after four days ($c_{4d} = 274.3 \pm 6.8$ µg mL^{-1}). In our hands, incubation for periods longer than four days did not yield consistent results, potentially due to oxidative degradation of hydrocortisone as reviewed by Gupta (1978).

The IDR is proportional to the equilibrium solubility (Mosharraf and Nyström, 1995; Surov et al., 2012); since there was no significant difference regarding the IDR of the two modifications, we assume that either there is no difference in thermodynamic solubility between HC and HC·MeOH or that the methanolate transforms to the non-solvate on the surface very quickly. The slower dissolution process observed during the equilibrium solubility experiment is thus regarded to be exclusively due to the smaller surface area of the large HC·MeOH crystals.

3.2. Combined dissolution/permeation experiments with methanolate tablets and permeation from hydrocortisone suspension

As intended, dissolution of all tablets was incomplete. All dissolution curves approached a plateau value once a dynamic equilibrium was reached between the amount dissolving and the amount permeating during each time interval. The highest plateau value was observed for the uncovered tablets without dilution, whereas the lowest value was observed for the tablets covered with paraffin; an intermediate value was reached in the case of the uncovered tablet where the donor was diluted through sampling (Fig. 1). Due to the area exposed to PBS being constant, the overall release rate from the covered tablets was likewise constant when also taking into account the permeated amount (Fig. 2).

The rank order observed for the dissolution profiles was the same as for the permeation profiles. All formulations exhibited non-linear permeation profiles during the first 3 h; a linear increase of the permeated amount was obtained once the dissolution profile started to approach the plateau value. In contrast, in the case of the saturated HC suspension, the cumulative amount permeated into the acceptor compartment increased linearly right from the beginning and showed the highest flux (Fig. 3). The constant flux indicated steady-state conditions, where the permeation across the barrier was rate-limiting.

Throughout all experiments, the concentration in the acceptor compartment was less than 10% of the donor concentration.

Based on the permeation experiment with the HC suspension at 37 °C, P_{app} was determined to be $2.71 \pm 0.24 \cdot 10^{-5}$ cm s^{-1}. In comparison, P_{app} determined under comparable conditions, but at 25 °C was $1.18 \pm 0.17 \cdot 10^{-5}$ cm s^{-1}, and hence, the permeability of HC across Permeapad® is clearly dependent on temperature.

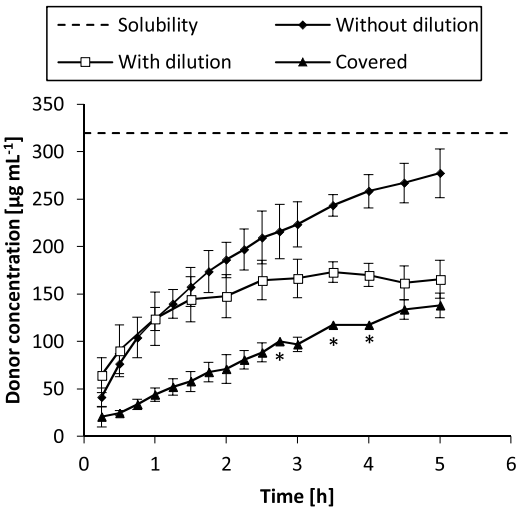

Fig. 1. Dissolution profiles of HC·MeOH tablets: uncovered tablets without dilution by sampling procedure (closed diamonds), uncovered tablets with dilution (open squares), and covered tablets without dilution (closed triangles). The dashed line represents the equilibrium solubility. Values are reported as mean ± S.D. (n = 3). *Mean value (n = 2).

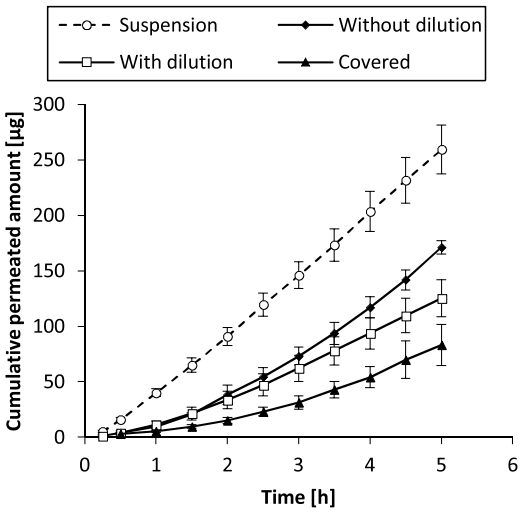

Fig. 3. Cumulative permeated amount from different formulations vs. time: uncovered tablets without dilution (closed diamonds), uncovered tablets with dilution (open squares), covered tablets without dilution (closed triangles), and suspension (open circles) (mean ± S.D., n = 3).

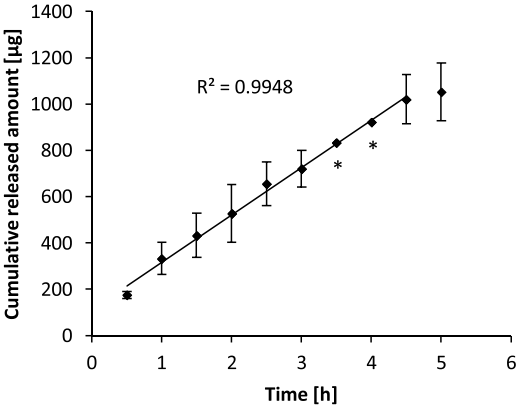

Fig. 2. Cumulative released amount from the covered tablets vs. time, calculated as the sum of the dissolved amount in the donor compartment and the permeated amount. Values are reported as mean ± S.D. (n = 3). *Outlier-corrected mean values.

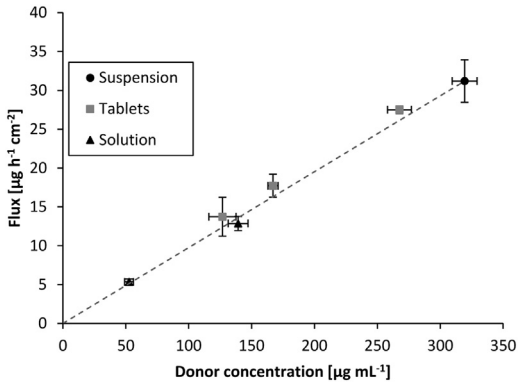

Fig. 4. Flux versus donor concentration for different permeation experiments: suspension (closed circle, mean ± S.D. of solubility), tablets (gray squares, mean ± S.D. of plateau concentration), and depletion experiments (closed triangles, mean ± S.D. of all donor concentrations) (n = 3–6). The dashed line represents the interpolation between the origin and the suspension.

3.3. Donor depletion experiments

It was the intention of these experiments to decrease the concentration in the donor compartment substantially over the course of the 6 h. However, despite a decrease by up to 20%, no decrease of permeation rate was observed. Instead, the cumulative permeated amount increased linearly, indicating steady state flux.

When looking at the different (dissolution/) permeation experiments, a linear correlation between donor concentration and flux was obtained, which is in line with Eq. (2). The suspension of micronized HC was taken as a reference since the concentration was constant throughout the experiment. All values from the combined dissolution/permeation and the depletion experiments were in good agreement with the interpolated line between the value measured for the suspension and the origin (Fig. 4).

3.4. Long-term depletion experiment

As opposed to the shorter depletion experiments, a substantial decrease of both donor concentration and flux was indeed observed when testing the permeation from a HC solution over a period of 94.5 h (Fig. 5). Over the course of the experiment, the donor concentration dropped by 96%. Accordingly, the flux value obtained at the last time point accounted for as little as 3% of the initial flux.

Based on Eq. (7), a P_{app} value of $3.55 \pm 0.32 \cdot 10^{-5}$ cm s^{-1} was calculated from the donor profile/exponential fit. From the acceptor profile, a P_{app} value of $3.36 \pm 0.28 \cdot 10^{-5}$ cm s^{-1} was calculated by dividing the flux at a specific time point by the donor concentration at the same time point (only values above the LOQ were included, i.e. until 41 h). As expected, there is no significant difference between the results ($p > 0.05$) and this experiment confirms the general concept of P_{app}. The quantitative P_{app} values found in this experiment where slightly higher than the value measured during the other experiments.

At the end of the experiment, approx. 13 µg of HC could be retrieved from the barrier by dissolving it in ethanol. The overall drug recovery was 89 ± 2% when taking into account the amount removed by sampling. The recovery calculated after 41 h (not taking into account HC accumulated in the barrier) was 93 ± 4%.

Finally, it should be noted that the decrease in the donor represented an exponential decay with a uniform decay-constant

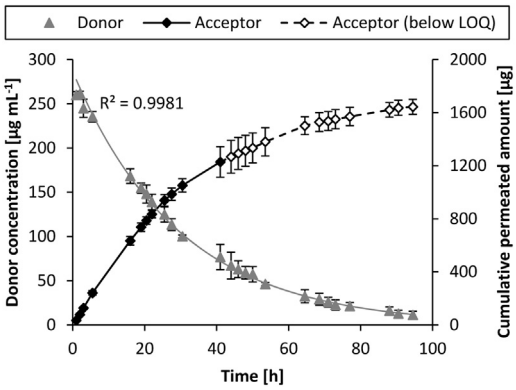

Fig. 5. Donor concentration (gray triangles) and permeated amount (closed diamonds) measured during long-term depletion experiment (mean ± S.D., n = 3). Acceptor values below the LOQ (hollow diamonds) are only reported for indicative reasons. The continuous gray line depicts the exponential fit, whereas the black lines are only meant to guide the eyes.

over the whole period of 94.5 h, indicating that the permeation properties of the biomimetic barrier Permeapad® stayed unchanged even during the long duration of the experiment. Permeapad® appears thus to be a good choice for long-term permeation experiments.

3.5. Prediction of permeation profiles

In general, the prediction of the acceptor profiles from the dissolution profiles was very good for the combined dissolution/permeation experiments in all cases where the donor was not diluted through the sampling procedure (Fig. 6). In the experiment with repeated dilution, the donor concentration follows a saw-tooth shaped curve. Even by correcting for this pattern in the calculation, a discrepancy between the calculated and the measured profile persists. The steep initial increase in concentration measured in the donor compartment is not reflected in the measured permeation profile and causes the horizontal shift of the predicted profile.

In absence of a mathematical model describing the interplay between the dissolution and the permeation process, interval-based derivation of the permeation profile from the dissolution profile appears to be a viable option for predicting the permeation profile in a dynamic setup (provided that sink conditions are given). However, this is only applicable to cases where the drug is either present as a solid or as truly dissolved drug, but not solubilized.

3.6. General considerations regarding the experimental setup

For developing a combined dissolution/permeation setup, the ratio between the area of the permeation barrier and the volume of the donor compartment contributes largely to the usefulness of the model. The area-to-volume ratio of the setup used in this study is 0.25 cm^2 mL^{-1} and, thus, in the same order of magnitude as other side-by-side setups described in literature (Table 2). However, it can be concluded from the present study that in order to achieve a substantial decrease in donor concentration within a reasonable period of time, higher ratios are necessary (unless the permeation rate can be increased by means other than an increased permeation area). This becomes even more obvious when considering that the flux decreases exponentially over time. An example: according to Eq. (7), an area-to-volume ratio of 5.9 cm^2 mL^{-1} would be necessary if 90% of the HC molecules in a donor solution should permeate across Permeapad® within 4 h.

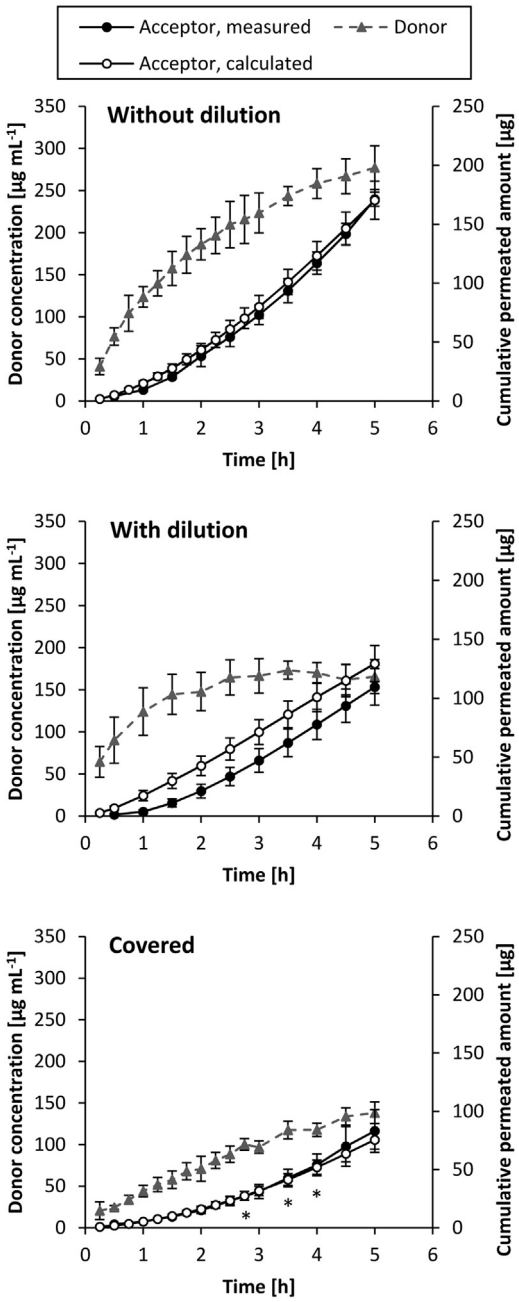

Fig. 6. Predicted (open circles) and measured (closed circles) permeation profiles and dissolution profiles (triangles) from different tablet formulations in combined dissolution/permeation studies (mean ± S.D., n = 3). *Outlier-corrected values.

However, if the drug first needs to dissolve (as it is the case with HC drug products *in vivo* and in dissolution/permeation studies), the concentration gradient will be even lower; consequently, even higher area-to-volume ratios are necessary.

4. Conclusion

In this study, we have experimentally demonstrated that the same correlation between drug concentration in the donor and passive diffusional flux of drug across the barrier applies for non-steady state conditions as is known for conventional permeability testing. Hence, the apparent permeability of a specific combination of drug and permeation barrier can be determined under steady

Table 2
Different dissolution/permeation setups described in literature and the respective area-to-volume ratio.

A [cm^2]	V_{Donor} [mL]	A/V [$cm^2\,mL^{-1}$]	Refs.
1.77	8	0.22	Kataoka et al. (2014)
1.13	>180[a]	<0.01	Gantzsch et al. (2014)
8.55	20	0.43	Borbás et al. (2015)
7.07	30	0.24	Raina et al. (2015)
1.13	12.5	0.09	Berthelsen et al. (2016)

[a] Flow-through setup.

state conditions (i.e. in a relatively simple experimental setup) and is still valid under more complex, non-steady state conditions.

Under the prerequisite that the drug concentration in the donor medium exclusively is defined as molecularly dissolved drug, the concept of apparent permeability can be employed for predicting the permeation profile from the donor profile in a dynamic setup. In cases where the apparent permeability is determined under conditions where part of the drug is solubilized (e.g. by components of the medium or by the formulation), this direct correlation of the profiles via the P_{app} value might not hold true; the distribution between the solubilized fraction and the free fraction might change over time, and this might result in the P_{app} value not being constant. In any case, due to the dynamic interplay of dissolution and permeation, only differential or – in a first approximation – interval-based derivation of the permeation profile from the dissolution profile seems appropriate.

Another experience from this study is that the area-to-volume ratio typically used in side-by-side setups is inappropriate to provoke a meaningful mutual influence between dissolution and permeation, as it would be needed for performance testing of enabling formulations. In this study, we had to reduce the dissolution rate deliberately in order to allow for such interplay between dissolution and permeation. For future dynamic dissolution/permeation studies, the aim obviously is to increase the permeation area while keeping the donor volume small in order to design an experimental setup in which substantial amounts can be transferred from the donor compartment to the acceptor compartment within a time interval that is realistic with respect to the dissolution rate of the formulation. Provided that P_{app} of a drug is known, this ratio might be a helpful indicator for estimating the usefulness of an experimental design.

Funding

This work was partly financed by AbbVie GmbH & Co. KG, D-67061 Ludwigshafen, Germany, as part of Daniel Sironi's PhD project.

Acknowledgement

We would like to thank stud. pharm. Ana Ventura (University of Porto) who helped with performing some of the experiments. Excellent technical support by Tina Christiansen is acknowledged.

References

Amidon, G.L., Lennernäs, H., Shah, V.P., Crison, J.R., Lennernäs, H., Shah, V.P., Crison, J. R., 1995. A theoretical basis for a biopharmaceutic drug classification: the correlation of in vitro drug product dissolution and in vivo bioavailability. Pharm. Res. 12, 413–420. doi:http://dx.doi.org/10.1023/A:1016212804288.

Artursson, P., 1990. Epithelial transport of drugs in cell culture. I: a model for studying the passive diffusion of drugs over intestinal absorptive (Caco-2) cells. J. Pharm. Sci. 79, 476–482. doi:http://dx.doi.org/10.1002/jps.2600790604.

Berthelsen, R., Byrialsen, J.P., Holm, R., Jacobsen, J., Abrahamsson, B., Saabye, L., Madelung, P., Müllertz, A., 2016. Development of a μdissolution-Permeation model with in situ drug concentration monitoring. J. Drug Deliv. Sci. Technol. 35, 223–233. doi:http://dx.doi.org/10.1016/j.jddst.2016.06.013.

Bevernage, J., Brouwers, J., Annaert, P., Augustijns, P., 2012. Drug precipitation-permeation interplay: supersaturation in an absorptive environment. Eur. J. Pharm. Biopharm. 82, 424–428. doi:http://dx.doi.org/10.1016/j.ejpb.2012.07.009.

Bibi, H.A., Holm, R., Bauer-Brandl, A., 2016. Use of Permeapad® for prediction of buccal absorption: a comparison to in vitro, ex vivo and in vivo method. Eur. J. Pharm. Sci. 93, 399–404. doi:http://dx.doi.org/10.1016/j.ejps.2016.08.041.

Blanquet, S., Zeijdner, E., Beyssac, E., Meunier, J.P., Denis, S., Havenaar, R., Alric, M., 2004. A dynamic artificial gastrointestinal system for studying the behavior of orally administrated drug dosage forms under various physiological conditions. Pharm. Res. 21, 585–591. doi:http://dx.doi.org/10.1023/B:PHAM.0000022404.70478.4b.

Borbás, E., Balogh, A., Bocz, K., Müller, J., Kiserdei, É., Vigh, T., Sinkó, B., Marosi, A., Halász, A., Dohányos, Z., Szente, L., Balogh, G.T., Nagy, Z.K., 2015. In vitro dissolution-permeation evaluation of an electrospun cyclodextrin-based formulation of aripiprazole using μFlux™. Int. J. Pharm. 491, 180–189. doi:http://dx.doi.org/10.1016/j.ijpharm.2015.06.019.

Buckley, S.T., Fischer, S.M., Fricker, G., Brandl, M., 2012. In vitro models to evaluate the permeability of poorly soluble drug entities: challenges and perspectives. Eur. J. Pharm. Sci. 45, 235–250. doi:http://dx.doi.org/10.1016/j.ejps.2011.12.007.

Chen, J., Wang, J., Ulrich, J., Yin, Q., Xue, L., 2008. Effect of solvent on the crystal structure and habit of hydrocortisone. Cryst. Growth Des. 8, 1490–1494. doi:http://dx.doi.org/10.1021/cg0703947.

Di Cagno, M., Bauer-Brandl, A., 2016. Assembly for drug permeability with adjustable biomimetic properties. WO 2016/078667 A1.

Di Cagno, M., Bibi, H.A., Bauer-Brandl, A., 2015. New biomimetic barrier Permeapad™ for efficient investigation of passive permeability of drugs. Eur. J. Pharm. Sci. 73, 29–34. doi:http://dx.doi.org/10.1016/j.ejps.2015.03.019.

FDA, 2015. Guidance for Industry: Waiver of in vivo bioavailability and bioequivalence studies for immediate-release solid oral dosage forms based on a biopharmaceutics classification system.

Fischer, S.M., Flaten, G.E., Hagesæther, E., Fricker, G., Brandl, M., 2011. In-vitro permeability of poorly water soluble drugs in the phospholipid vesicle-based permeation assay: the influence of nonionic surfactants. J. Pharm. Pharmacol. 63, 1022–1030. doi:http://dx.doi.org/10.1111/j.2042-7158.2011.01301.x.

Fischer, S.M., Buckley, S.T., Kirchmeyer, W., Fricker, G., Brandl, M., 2012. Application of simulated intestinal fluid on the phospholipid vesicle-based drug permeation assay. Int. J. Pharm. 422, 52–58. doi:http://dx.doi.org/10.1016/j.ijpharm.2011.10.026.

Flaten, G.E., Luthman, K., Vasskog, T., Brandl, M., 2008. Drug permeability across a phospholipid vesicle-based barrier 4. The effect of tensides, co-solvents and pH changes on barrier integrity and on drug permeability. Eur. J. Pharm. Sci. 34, 173–180. doi:http://dx.doi.org/10.1016/j.ejps.2008.04.001.

Fong, S.Y.K., Poulsen, J., Brandl, M., Bauer-Brandl, A., 2017. A novel microdialysis-dissolution/permeation system for testing oral dosage forms: a proof-of-concept study. Eur. J. Pharm. Sci. 96, 154–163. doi:http://dx.doi.org/10.1016/j.ejps.2016.09.018.

Frank, K.J., Locher, K., Zecevic, D.E., Fleth, J., Wagner, K.G., 2014. In vivo predictive mini-scale dissolution for weak bases: advantages of pH-shift in combination with an absorptive compartment. Eur. J. Pharm. Sci. 61, 32–39. doi:http://dx.doi.org/10.1016/j.ejps.2013.12.015.

Gantzsch, S.P., Kann, B., Ofer-Glaessgen, M., Loos, P., Berchtold, H., Balbach, S., Eichinger, T., Lehr, C.M., Schaefer, U.F., Windbergs, M., 2014. Characterization and evaluation of a modified PVPA barrier in comparison to Caco-2 cell monolayers for combined dissolution and permeation testing. J. Control. Release 175, 79–86. doi:http://dx.doi.org/10.1016/j.jconrel.2013.12.009.

Ginski, M.J., Polli, J.E., 1999. Prediction of dissolution-absorption relationships from a dissolution/Caco-2 system. Int. J. Pharm. 177, 117–125. doi:http://dx.doi.org/10.1016/s0378-5173(98)00330-5.

Ginski, M.J., Taneja, R., Polli, J.E., 1999. Prediction of dissolution-absorption relationships from a continuous dissolution/Caco-2 system. AAPS PharmSci 1, 27–38. doi:http://dx.doi.org/10.1208/ps010203.

Gupta, V.D., 1978. Effects of vehicles and other active ingredients on stabillity of hydrocortisone. J. Pharm. Sci. 67, 299–302. doi:http://dx.doi.org/10.1002/jps.2600670305.

Kataoka, M., Masaoka, Y., Yamazaki, Y., Sakane, T., Sezaki, H., Yamashita, S., 2003. In vitro system to evaluate oral absorption of poorly water-soluble drugs: simultaneous analysis on dissolution and permeation of drugs. Pharm. Res. 20, 1674–1680. doi:http://dx.doi.org/10.1023/A:1026107906191.

Kataoka, M., Masaoka, Y., Sakuma, S., Yamashita, S., 2006. Effect of food intake on the oral absorption of poorly water-soluble drugs: in vitro assessment of drug dissolution and permeation assay system. J. Pharm. Sci. 95, 2051–2061. doi:http://dx.doi.org/10.1002/jps.20691.

Kataoka, M., Itsubata, S., Masaoka, Y., Sakuma, S., Yamashita, S., 2011. In vitro dissolution/permeation system to predict the oral absorption of poorly water-soluble drugs: effect of food and dose strength on it. Biol. Pharm. Bull. 34, 401–407. doi:http://dx.doi.org/10.1248/bpb.34.401.

Kataoka, M., Tsuneishi, S., Maeda, Y., Masaoka, Y., Sakuma, S., Yamashita, S., 2014. A new in vitro system for evaluation of passive intestinal drug absorption: establishment of a double artificial membrane permeation assay. Eur. J. Pharm. Biopharm. 88, 840–846. doi:http://dx.doi.org/10.1016/j.ejpb.2014.09.009.

Ku, M.S., Dulin, W., 2012. A biopharmaceutical classification based Right First Time formulation approach to reduce human pharmacokinetic variability and project cycle time from First-In-Human to clinical Proof-Of-Concept. Pharm. Dev. Technol. 17, 285–302. doi:http://dx.doi.org/10.3109/10837450.2010.535826.

Lovering, E.G., Black, D.B., 1973. Drug permeation through membranes I: effect of various substances on amobarbital permeation through polydimethylsiloxane. J. Pharm. Sci. 62, 602–606. doi:http://dx.doi.org/10.1002/jps.2600620412.

Mosharraf, M., Nyström, C., 1995. The effect of particle size and shape on the surface specific dissolution rate of microsized practically insoluble drugs. Int. J. Pharm. 122, 35–47. doi:http://dx.doi.org/10.1016/0378-5173(95)00033-F.

Motz, S.A., Schaefer, U.F., Balbach, S., Eichinger, T., Lehr, C.M., 2007. Permeability assessment for solid oral drug formulations based on Caco-2 monolayer in combination with a flow through dissolution cell. Eur. J. Pharm. Biopharm. 66, 286–295. doi:http://dx.doi.org/10.1016/j.ejpb.2006.10.015.

Phillips, D.J., Pygall, S.R., Cooper, V.B., Mann, J.C., 2012. Overcoming sink limitations in dissolution testing: a review of traditional methods and the potential utility of biphasic systems. J. Pharm. Pharmacol. 64, 1549–1559. doi:http://dx.doi.org/10.1111/j.2042-7158.2012.01523.x.

Raina, S.A., Zhang, G.G.Z., Alonzo, D.E., Wu, J., Zhu, D., Catron, N.D., Gao, Y., Taylor, L. S., 2015. Impact of solubilizing additives on supersaturation and membrane transport of drugs. Pharm. Res. 32, 3350–3364. doi:http://dx.doi.org/10.1007/s11095-015-1712-4.

Sironi, D., Rosenberg, J., Bauer-Brandl, A., Brandl, M., 2017. Dynamic dissolution-/permeation-testing of nano- and microparticle formulations of fenofibrate. Eur. J. Pharm. Sci. 96, 20–27. doi:http://dx.doi.org/10.1016/j.ejps.2016.09.001.

Surov, A., Solanko, K., Bond, A., Perlovich, G., Bauer-Brandl, A., 2012. Crystallization and polymorphism of felodipine. Cryst. Growth Des. 12, 4022–4030. doi:http://dx.doi.org/10.1016/j.tca.2013.01.013.